State Estimation of Common Emitter Amplifier using Iterated Extended Kalman Filters

Amit Kumar Gautam, Sudipta Majumdar

Abstract*: This paper presents the output voltage estimation of bipolar junction transistor (BJT) common emitter (CE) using iterated extended Kalman filter (IEKF). For this, state space model has been derived using Kirchhoff's current law (KCL) and Ebers-Moll model of the transistor. The performance of IEKF has been compared with extended Kalman filter (EKF). The simulation results show large signal to noise ratio (SNR) and small root mean square error (RMSE) using IEKF as compared to EKF, as IEKF considers the error due to linearization. The advantage of the proposed method is that the derived extended state space equation can be used for parameter estimation of both, the transistor state and transistor parameters as the derivation includes transistor model.

Index Terms*: Ebers-Moll model, extended Kalman filter, iterated extended Kalman filter, Kirchhoff's current law, state space model.

I. INTRODUCTION

Bipolar junction transistor (BJT) common emitter (CE) is an important circuit component of different electronic circuits and chips. It is widely used in wideband resistive feedback low noise amplifier (LNA) [1], two cascaded common base and common emitter devices [2], frequency reconfigurable millimeter wave power amplifier (PA) [3], transimpedance amplifier circuit [4], class-F PA [5] and in dual-vector phase rotator (DVR) used to drive a Dohetry amplifier in beamformer [6]. BJT CE circuit is also used in monolithic microwave integrated circuit chip [7] and in transimpedance amplifier used in optical network link [8].

Various versions of Kalman filter (KF) have been used for state estimation in many applications. In [9], KF has been used for optimal estimation of noise corrupted input and output. In [10], KF and adaptive KF have been used to obtain the fault type and location of digital protection schemes. In [11], Crouse *et al.* proposed moving horizon Kalman finite impulse response (FIR) smoother which has the advantage of simple recursive calculation. It also permits the use of control input. In [12], Sarmavuori *et al.* proposed Fourier-Hermite KF. This is based on Fourier-Hermite series as the EKF is based on Taylor series. The main advantage of the method is that due to the orthogonality of the Hermite polynomials, the truncation is easier as compared to Taylor series truncation. In [13], Hong *et al.* proposed a filtering method based on wavelets and used KF for multiresolution decomposition and estimation. In [14], Jose *et al.* used tuning KF for proper tracking of harmonic fluctuation which has the advantage of fast adaptivity for abrupt input changes. The disadvantage of KF is that it cannot be used for nonlinear systems. For nonlinear systems, the EKF has been proposed which is based on the linearization of nonlinear function using Taylor series. EKF and its variants have been used in different applications, In [15], Reggiani *et al.* used EKF for phase noise estimation of multi-input multi output transmission. Reif *et al.* [16] used EKF as a state estimation for nonlinear deterministic system and showed that the estimation error is exponentially stable. Carlos *et al.* [17] studied the behaviour of EKF for chaotic signals. Shmaliy [18] proposed nonlinear extended finite impulse response filters which does not require the noise statistics and initial error. EKF has the disadvantage of large linearization error which may lead in wrong estimations. To reduce the linearization error, IEKF has been proposed in the literature and used for various applications [19]-[22]. The paper is organized as follows. Section II gives brief theory of EKF. Section III presents IEKF method. Section IV presents state modeling of CE amplifier circuit using Kirchhoff's law and transistor model. Section V presents implementation of EKF and IEKF to CE amplifier circuit. Section VI presents simulation results. Section VI concludes the paper.

II. EXTENDED KALMAN FILTER

EKF [23], [24] is an extended version of Kalman filter that is used for nonlinear systems. It consists of three steps. After initialization, it is an iterative process between time update and measurement update. Representing the nonlinear system using

$$x_k = f_{k-1}(x_{k-1}, u_{k-1}) + w_{k-1} \quad (1)$$

$$y_k = h_k(x_k) + v_k \quad (2)$$

where x_k is the system state vector to be estimated at time k. u_k is a known input vector, y_k is measurement vector. $f_k(.)$ and $h_k(.)$ are nonlinear functions known as state transition function and measurement function respectively. w_k and v_k are process and measurement noise with zero mean and covariances Q_k and R_k respectively.

EKF uses Taylor's series expansion to linearize the nonlinear function $f_k(.)$ and $h_k(.)$. (1) and (2) has been approximated using

Revised Manuscript Received on July 07, 2019.

Amit Kumar Gautam, Department of Electronics and Communiation Engineering, Delhi Technological University, Delhi, India.
Sudipta Majumdar, Department of Electronics and Communiation Engineering, Delhi Technological University, Delhi, India.

Taylor's series expansion as:

$$x_k = f_{k-1}(\hat{x}_{k-1|k-1}) + F_{k-1}\%_{k-1} + \text{Higher order terms} \quad (3)$$

$$y_k = h_k(f_{k-1}(\hat{x}_{k-1|k-1})) + H_k\%_{k-1} + \text{Higher order terms} \quad (4)$$

where F_k and H_k denote the Jacobian matrices calculated by partial derivative of $f_k(.)$ and $h_k(.)$ with respect to state x_i.

$$F_k = \frac{\partial f_i(x,u_k)}{\partial x_j}|_{x=\hat{x}_{k|k-1}} \quad (5)$$

$$H_k = \frac{\partial h_i(x,u_k)}{\partial x_j}|_{x=\hat{x}_{k|k}} \quad (6)$$

The steps involved for EKF algorithm are as follows:

1) Initialization Step: This step initializes

$\hat{x}_0 = \mu_0 = E[x_0]$,

$P_0 = E[(x_0 - \hat{x}_0)(x_0 - \hat{x}_0)^T]$, Q_k and R_k.

2) State prediction: State $\hat{x}$ and covariance matrix $P_{k|k-1}$ are obtained using following expressions:

a) Predicted state $\hat{x}_{k|k-1}$ is computed as

$$\hat{x}_{k|k-1} = F_k\hat{x}_{k-1|k-1} + B_k u_k \quad (7)$$

where

$$B_k = \frac{\partial f_i(x,u_k)}{\partial x_j}|_{x=u_k} \quad (8)$$

b) The covariance matrix of prediction error is computed using

$$P_{k|k-1} = F_k P_{k-1|k-1} F_k^T + Q_{k-1} \quad (9)$$

3) Measurement update: In the measurement step, the state covariance matrix is updated by Kalman gain. This step computes following three parameters:

a) This step calculates H_k and Kalman gain as:

$$K_k = P_{k|k-1}H_k^T(H_k P_{k|k-1} H_k^T + R_k)^{-1} \quad (10)$$

b) This step updates the state estimation using the following expression

$$\hat{x}_{k|k} = \hat{x}_{k|k-1} + K_k(y_k - h_k(\hat{x}_{k|k-1})) \quad (11)$$

c) This step computes covariance error matrix using the following equation

$$P_{k|k} = (I - K_k H_k)P_{k|k-1} \quad (12)$$

and repeat step 2. $k|k-1$ and $k|k$ are a prior and a post estimate.

III. ITERATIVE EXTENDED KALMAN FILTER

In the IEKF [24], the linearization of f, $\hat{x}_{k|k-1}$ and $P_{k|k-1}$ are done as in EKF method. The only difference between both approaches is that in IEKF, linearization of g depends on the updated state estimate $\hat{x}_{k|k}$ rather than the predicted state estimate $\hat{x}_{k|k-1}$ as the EKF does. Measurement model is defined as:

$$v_k = h_k(y_k, x_k) \quad (13)$$

where $h_k(.)$ denotes a function. In case of additive white noise, the measurement model is

$$y_k = g_k(x_k) + G_k v_k \quad (14)$$

and therefore

$$v_k = (G_k)^{-1}(y_k - g_k(x_k)) \quad (15)$$

where G_k denotes the invertible matrix and g_k is nonlinear function. IEKF method has following steps:

a) In this step, threshold value is set (denoted as ε) and $\hat{x}_{k|k-1}$, $P_{k|k-1}$ and R_k are computed.

b) Counter $i = 0$ is set. Updated estimate is calculated using $\hat{x}_{k|k}$ at $i = 0$.

c)

1) In this step, counter is incremented $i = i + 1$.
2) This step performs the linearization of the model as $H_k^{\ i} = \frac{dg_k}{dx}(y_k, \hat{x}_{k|k}^{i-1})$
3) This step computes the Kalman gain as:

$$K_k^i = P_{k|k-1}(H_k^i)^T(H_k^i P_{k|k-1}(H_k^i)^T + R_k)^{-1} \quad (16)$$

d)

1) This step estimates updated state as:

$$\hat{x}_{k|k}^i = \hat{x}_{k|k-1} - K_k^i(h_k(y_k, \hat{x}_{k|k}^{i-1}) - G_k^i(\hat{x}_{k|k-1} - \hat{x}_{k|k}^{i-1})) \quad (17)$$

2) This process is repeated untill

$$\| (\hat{x}_{k|k}^i - \hat{x}_{k|k}^{i-1}) \| < \varepsilon \quad (18)$$

Set $i = 0$ and $\hat{x}_{k|k} - \hat{x}_{k|k}^{i_0}$

3) This step updated state as:

$$(\hat{x}_{k|k} = \hat{x}_{k|k}^{i_0}) \quad (19)$$

4) This step update the covariance of estimate as:

$$P_{k|k} = (I - K_k^{i_0} G_k^{i_0})P_{k|k-1} \quad (20)$$

IV. MATHEMATICAL MODELING OF COMMON EMITTER AMPLIFIER CIRCUIT

The CE transistor amplifier is shown in Fig. 1.

It consists of resistors R_C, R_E, R_1, and R_L. Capacitor C_B is used to block dc voltage only. C_C and C_E are the collector and emitter capacitors respectively. u and v_0 denote the input and output voltage of the amplifier circuit respectively.

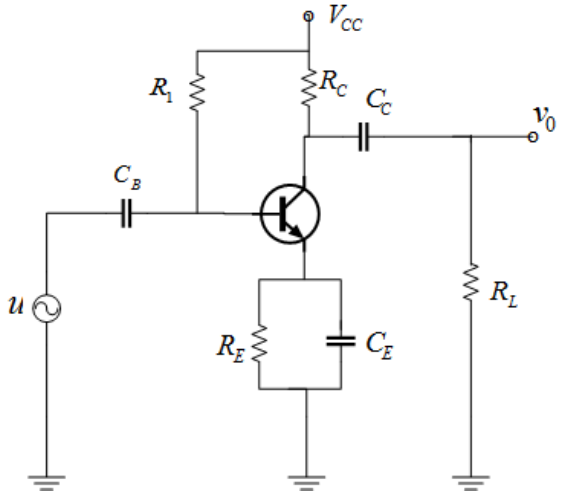

Fig. 1 Circuit diagram of common emitter amplifier.

Applying KCL, we obtain the following equations:

$$I_E = C_E \frac{d}{dt} v_E + \frac{v_E}{R_E} \tag{21}$$

$$I_B = C_B \frac{d}{dt}(u - v_B) + \frac{V_{CC} - v_B}{R_1} \tag{22}$$

$$C_C \frac{d}{dt}(v_C - v_0) = \frac{v_0}{R_L} \tag{23}$$

$$\frac{V_{CC} - v_C}{R_C} = I_C + \frac{v_0}{R_L} \tag{24}$$

These equations can be expressed in terms of state variables namely v_E, v_B, v_C and v_0. We used Ebers-Moll model [25] to obtain the state space equations. Ebers-Moll equations are:

$$I_E = -I_{ES}\left\{\exp\left(\frac{v_{BE}}{V_T}\right) - 1\right\} + \alpha_R I_{CS}\left\{\exp\left(\frac{v_{BC}}{V_T}\right) - 1\right\} \tag{25}$$

$$I_C = -I_{CS}\left\{\exp\left(\frac{v_{BC}}{V_T}\right) - 1\right\} + \alpha_F I_{ES}\left\{\exp\left(\frac{v_{BE}}{V_T}\right) - 1\right\} \tag{26}$$

where

I_E = Emitter current

I_C = Collector current

I_{ES} = Saturation current for emitter junctions

I_{CS} = Saturation current for collector junctions

α_F = Forward current gain

α_R = Reverse current gain

V_T = Thermal voltage.

(25) and (26) can be expanded using Taylor's series expansion as:

$$I_E = K_1 v_E + K_2 v_B + K_3 v_C + K_4 v_E v_E + K_5 v_B v_B + K_6 v_C v_C + K_7 v_B v_E + K_8 v_B v_C \tag{27}$$

$$I_C = K_9 v_E + K_{10} v_B + K_{11} v_C + K_{12} v_E v_E + K_{13} v_B v_B + K_{14} v_C v_C + K_{15} v_B v_E + K_{16} v_B v_C \tag{28}$$

$$I_B = (K_1 - K_9) v_E + (K_2 - K_{10}) v_B + (K_3 - K_{11}) v_C + (K_4 - K_{12}) v_E v_E + (K_5 - K_{13}) v_B v_B + (K_6 - K_{14}) v_C v_C + (K_7 - K_{15}) v_B v_E + (K_8 - K_{16}) v_B v_C \tag{29}$$

where

$$K_1 = \frac{I_{ES}}{V_T}, \qquad K_2 = -\frac{I_{ES} - \alpha_R I_{CS}}{V_T},$$

$$K_3 = -\frac{\alpha_R I_{CS}}{V_T}, \qquad K_4 = -\frac{I_{ES}}{2V_T^2},$$

$$K_5 = -\frac{I_{ES} - \alpha_R I_{CS}}{2V_T^2}, \qquad K_6 = \frac{\alpha_R I_{CS}}{2V_T^2},$$

$$K_7 = \frac{I_{ES}}{V_T^2}, \qquad K_8 = -\frac{\alpha_R I_{CS}}{V_T^2},$$

$$K_9 = \frac{-\alpha_F I_{ES}}{V_T}, \qquad K_{10} = \frac{\alpha_F I_{ES} - I_{CS}}{V_T},$$

$$K_{11} = \frac{I_{CS}}{V_T}, \qquad K_{12} = \frac{\alpha_F I_{ES}}{2V_T^2},$$

$$K_{13} = \frac{\alpha_F I_{ES} - I_{CS}}{2V_T^2}, \qquad K_{14} = \frac{-I_{CS}}{2V_T^2},$$

$$K_{15} = \frac{-\alpha_F I_{ES}}{V_T^2}, \qquad K_{16} = \frac{I_{CS}}{V_T^2}.$$

Substituting (27)-(29) in (21)-(24), we obtain the following state space equations:

$$\frac{dv_E}{dt} = K_{17} v_E + K_{18} v_B + K_{19} v_C + K_{20} v_E v_E + K_{21} v_B v_B + K_{22} v_C v_C + K_{23} v_B v_E + K_{24} v_B v_C \tag{30}$$

$$\frac{dv_B}{dt} = K_{25} v_E + K_{26} v_B + K_{27} v_C + K_{28} v_E v_E + K_{29} v_B v_B + K_{30} v_C v_C + K_{31} v_B v_E + K_{32} v_B v_C + u' + K_{33} V_{CC} \tag{31}$$

$$\frac{dv_C}{dt} = K_{34} v_E + K_{35} v_B + K_{36} v_C + K_{37} v_0 + K_{38} v_E v_E + K_{39} v_B v_B + K_{40} v_C v_C + K_{41} v_B v_E + K_{42} v_B v_C \tag{32}$$

$$\frac{dv_0}{dt} = K_{34} v_E + K_{35} v_B + K_{36} v_C + K_{43} v_0 + K_{38} v_E v_E + K_{39} v_B v_B + K_{40} v_C v_C + K_{41} v_B v_E + K_{42} v_B v_C \tag{33}$$

where $u' = \frac{d}{dt} u$.

$$K_{17}=\frac{1}{C_E}\left(K_1-\frac{1}{R_E}\right), \qquad K_{18}=\frac{K_2}{C_E},$$

$$K_{19}=\frac{K_3}{C_E}, \qquad K_{20}=\frac{K_4}{C_E},$$

$$K_{21}=\frac{K_5}{C_E}, \qquad K_{22}=\frac{K_6}{C_E},$$

$$K_{23}=\frac{K_7}{C_E}, \qquad K_{24}=\frac{K_8}{C_E},$$

$$K_{25}=\frac{K_9-K_1}{C_B}, \qquad K_{26}=\frac{1}{C_B}\left(K_{10}-K_2+\frac{1}{R_1}\right),$$

$$K_{27}=\frac{K_{11}-K_3}{C_B}, \qquad K_{28}=\frac{K_{12}-K_4}{C_B},$$

$$K_{29}=\frac{K_{13}-K_5}{C_B}, \qquad K_{30}=\frac{K_{14}-K_6}{C_B},$$

$$K_{31}=\frac{K_{15}-K_7}{C_B}, \qquad K_{32}=\frac{K_{16}-K_8}{C_B},$$

$$K_{33}=\frac{1}{C_B R_1}, \qquad K_{34}=\frac{-\alpha_F R_L R_C}{C_E Z_E}\left(K_1-\frac{1}{R_E}\right),$$

$$K_{35}=\frac{-\alpha_F R_L R_C K_2}{C_E Z_E}, \qquad K_{36}=\frac{-\alpha_F R_L R_C K_3}{C_E Z_E},$$

$$K_{37}=\frac{R_C}{R_L(R_L+R_C)}, \qquad K_{38}=\frac{-\alpha_F R_L R_C K_4}{C_E Z_E},$$

$$K_{39}=\frac{-\alpha_F R_L R_C K_5}{C_E Z_E}, \qquad K_{40}=\frac{-\alpha_F R_L R_C K_6}{C_E Z_E},$$

$$K_{41}=\frac{-\alpha_F R_L R_C K_7}{C_E Z_E}, \qquad K_{42}=\frac{-\alpha_F R_L R_C K_8}{C_E Z_E},$$

$$K_{43}=\frac{1}{C_C(R_L+R_C)}. \tag{34}$$

The state space model can be represented as:

$$x_k=F_{k-1}x_{k-1}+B_k u_{k-1}+w_{k-1} \tag{35}$$

$$y_k=H_k x_k+v_k \tag{36}$$

x_k denotes the state vector and B_k is the input vector. They are:

$$x_k=\begin{bmatrix}v_E(k) & v_B(k) & v_C(k) & v_0(k)\end{bmatrix}^T \tag{37}$$

$$B_k=\begin{bmatrix}0 & 1 & 0 & 0\end{bmatrix}^T \tag{38}$$

where

w_k and v_k are the system and measurement noise. F_k is calculated by partial derivative of nonlinear function $f(.)$ to estimated states x as:

$$F_k=\frac{d}{dx}f(x_k,u_k)=\begin{bmatrix}F_{11} & F_{12} & F_{13} & F_{14}\\ F_{21} & F_{22} & F_{23} & F_{24}\\ F_{31} & F_{32} & F_{33} & F_{34}\\ F_{41} & F_{42} & F_{43} & F_{44}\end{bmatrix} \tag{39}$$

where

$$\begin{aligned}
F_{11}&=1+K_{17}+K_{20}v_E(k-1),\\
F_{12}&=K_{18}+K_{21}v_B(k-1)+K_{23}v_E(k-1),\\
F_{13}&=K_{19}+K_{22}v_C(k-1)+K_{24}v_B(k-1),\\
F_{14}&=0,\\
F_{21}&=K_{25}+K_{28}v_E(k-1),\\
F_{22}&=1+K_{26}+K_{29}v_B(k-1)+K_{31}v_E(k-1),\\
F_{23}&=K_{27}+K_{30}v_C(k-1)+K_{32}v_B(k-1),\\
F_{24}&=0,\\
F_{31}&=K_{34}+K_{38}v_E(k-1),\\
F_{32}&=K_{35}+K_{39}v_B(k-1)+K_{41}v_E(k-1),\\
F_{33}&=1+K_{36}+K_{40}v_C(k-1)+K_{42}v_B(k-1),\\
F_{34}&=K_{37},\\
F_{41}&=K_{34}+K_{38}v_E(k-1),\\
F_{42}&=K_{35}+K_{39}v_B(k-1)+K_{41}v_E(k-1),\\
F_{43}&=K_{36}+K_{40}v_C(k-1)+K_{42}v_B(k-1),\\
F_{44}&=1+K_{43},
\end{aligned} \tag{40}$$

The combined state space model is given as

$$\begin{bmatrix}v_E(k)\\ v_B(k)\\ v_C(k)\\ v_0(k)\end{bmatrix}=\begin{bmatrix}F_{11} & F_{12} & F_{13} & F_{14}\\ F_{21} & F_{22} & F_{23} & F_{24}\\ F_{31} & F_{32} & F_{33} & F_{34}\\ F_{41} & F_{42} & F_{43} & F_{44}\end{bmatrix}\begin{bmatrix}v_E(k-1)\\ v_B(k-1)\\ v_C(k-1)\\ v_0(k-1)\end{bmatrix}+\begin{bmatrix}0\\1\\0\\0\end{bmatrix}u'(k-1) \tag{41}$$

The measurement model is:

$$y_k=H_k x_k \tag{42}$$

where

$$H_k=\frac{d}{dx}h(x_k,u_k)=\begin{bmatrix}0 & 0 & 0 & 1\end{bmatrix} \tag{43}$$

V. APPLYING EKF AND IEKF TO THE COMMON EMITTER AMPLIFIER CIRCUIT

To implement EKF, the following steps have been used:

1) Initialization step:

After initializing Q_0, R_0, P_0 and state vector, we used following steps.

2) **State prediction:** We calculated state, F_k using (39) and compute covariance matrix of prediction error using (9).

3) **Measurement update:** For this, H_k has been calculated using (43) to compute Kalman gain, measurement update and error covariance.

To implement IEKF, first threshold value ε is set to a small value. Counter $i = 0$ is set. Then, the estimate state $\hat{x}$ is computed. Counter i is incremented. Then, Kalman gain and state update is computed using (16) and (17) respectively until (18) is satisfied. Finally, at this counter value i, covariance error is computed using (20).

VI. SIMULATION RESULTS

The derived equations have been implemented in MATLAB software. For simulations, following circuit components and parameter values have been used:

$R_1 = 100K\Omega$, $R_C = 10K\Omega$, $R_E = 6K\Omega$, $R_L = 5K\Omega$, $C_B = 10\mu F$, $C_C = 10\mu F$, $C_E = 10\mu F$, $\alpha_F = 0.98$, $\alpha_R = 0.25$, $\alpha_F = 0.98$, $I_{ES} = 1\times10^{-15}$, $I_{CS} = 1\times10^{-13}$, $V_T = 0.026V$, $V_{CC} = 20V$.

Two different scenarios have been considered here:- (i) estimation without noisy input and (ii) estimation with noisy input. Input signal is shown in Fig. 2. Sinusoidal signal of amplitude 1 V and frequency 10 KHz with sample step size 0.1 has been applied at the input. Then, noisy input has been used for output voltage estimation of BJT CE circuit. For this, white Gaussian noise of zero mean and different variances has been added. The process noise and measurement noise used are white Gaussian noise with zero mean and variances 0.5 and 0.01 respectively. For different noise values, SNR has been calculated using following expression:

$$RMSE = \sqrt{\frac{\sum_{i=1}^{n}(\hat{y}_i - y_i)^2}{n}} \quad (44)$$

$$SNR = 10log_{10}\left[\frac{\sum_{i=1}^{n}(\hat{y}_i)^2}{\sum_{i=1}^{n}(\hat{y}_i - y_i)^2}\right] \quad (45)$$

where y_i and $\hat{y}_i$ are the actual value and estimated value.

Table I presents the SNR for EKF and IEKF method for noiseless input. Table II presents the root mean square (RMS) error for both methods for noiseless input. Fig. 3 shows estimated output for noiseless input using IEKF and EKF method. Fig. 4 shows the estimated output for noisy input using IEKF and EKF method and compared with simulated values.

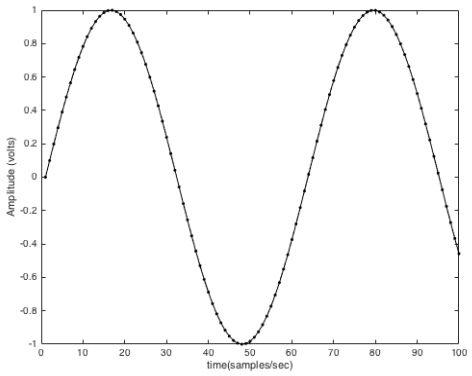

Fig. 2 Sinusoidal input.

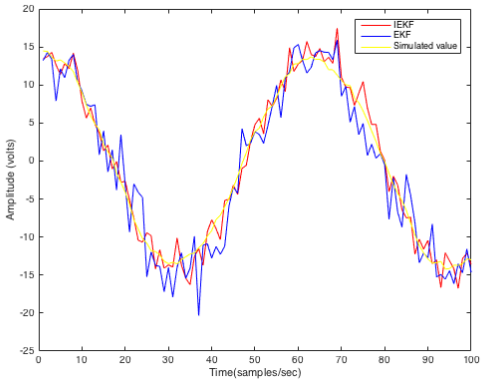

Fig. 3 Comparison of estimated output by IEKF and EKF method for noiseless input with PSPICE simulation.

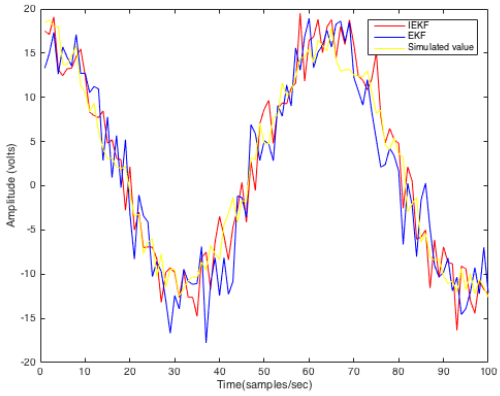

Fig. 4 Comparison of estimated output by IEKF and EKF method for noisy input with PSPICE simulation.

Table I: Comparison of SNR value using EKF and IEKF methods.

Noise Variance (σ^2)	SNR by EKF (dB)	SNR by IEKF (dB)
0.5	33.34	34.86
1.0	27.82	28.43
5.0	15.17	15.68
10.0	8.51	9.56

Table II: Comparison of parameters using EKF and IEKF methods.

Parameter	EKF	IEKF
Computation Time (Sec.)	4.04	2.28
RMS Error Value (dB)	78.1	73.9

VII. CONCLUSIONS

This paper estimated the output voltage of BJT CE circuit using IEKF and compares the performance of IEKF with EKF method. MATLAB simulations show that IEKF gives better SNR as compared to EKF, as IEKF reduces the linearization error by considering the measurement during linearization of measurement model. Also, in EKF method, due to linearization of nonlinear systems around the operating point of states, performance and stability is not assured for all operating conditions. The derived extended state equation can be used for estimation of both, the transistor states and transistor model parameters. Fig. 3 and 4 show that IEKF has better ability to track the state as compared to EKF because of linearization error consideration by IEKF.

Acknowledgement

First author thanks to UGC India.

REFERENCES

1. S. Zeinolabedinzadeh, A. C. Ulusoy, M. A. Oakley, N. E. Lourenco and J. D. Cressler, "A 0.3-15 GHz SiGe LNA With > 1 THz Gain-Bandwidth Product," *IEEE Microwave and Wireless Components Letters*, Vol. 27, No. 4, 2017, pp. 380-382.
2. S. Zeinolabedinzadeh, H. Ying, Z. E. Fleetwood, N. J. Roche, A. Khachatrian, D. McMorrow, S. P. Buchner, J. H. Warner, P. Paki-Amouzou and J. D. Cressler, "Single-Event Effects in High-Frequency Linear Amplifiers Experiment and Analysis," *IEEE Transactions on Nuclear Science*, Vol. 64, No. 1, 2017, pp. 125-132.
3. C. R. Chappidi and K. Sengupta, "Frequency Reconfigurable mm-Wave Power Amplifier with Active Impedance Synthesis in an Asymmetrical Non-Isolated Combiner: Analysis and Design," *IEEE Journal of Solid-State Circuits*, Vol. 52, No. 8, 2017, pp. 1990-2008.
4. S. P. Voinigescu, S. Shopov, J. Bateman, H. Farooq, J. Hoffman and K. Vasilakopoulos, "Silicon Millimeter-Wave, Terahertz, and High-Speed Fiber-Optic Device and Benchmark Circuit Scaling Through the 2030 ITRS Horizo," *Proceedings of the IEEE*, Vol. 105, No. 6, 2017, pp. 1087-1104.
5. S. Y. Mortazavi and K. J. Koh, "Integrated Inverse Class-F Silicon Power Amplifiers for High Power Efficiency at Microwave and mm-Wave," *IEEE Journal of Solid-State Circuits*, Vol. 51, No. 10, 2016, pp. 2420-2434.
6. K. Greene, A. Sarkar and B. Floyd, "A 60-GHz Dual-Vector Doherty Beamformer," *IEEE Journal of Solid-State Circuits*, Vol. 52, No. 5, 2017, pp. 1373-1387.
7. M. D. Luong, R. Ishikawa, Y. Takayama and K. Honjo, "Microwave Characteristics of an Independently Biased 3-Stack InGaP/GaAs HBT Configuration," *IEEE Transactions on Circuits and Systems I*, Vol. 64, No. 5, 2017, pp. 1140-1151.
8. B. Moeneclaey, F. Blache, J. V. Kerrebrouck, R. Brenot, G. Coudyzer, M. Achouche, X. Z. Qiu, J. Bauwelinck and X. Yin, "40-Gb/s TDM-PON Downstream Link With Low-Cost EML Transmitter and APD-Based Electrical Duobinary Receiver," *Journal of Lightwave Technolog*, Vol. 35, No. 4, 2017, pp. 1083-1089.
9. R. Diversi, R. Guidorzi and U. Soverini, "Kalman filtering in extended noise environments," *IEEE Transactions on Automatic Control*, Vol. 50, No. 9, 2005, pp.1396-402.
10. A. A. Girgis and D. G. Hart, "Implementation of Kalman and adaptive Kalman filtering algorithms for digital distance protection on a vector signal processor," *IEEE Transactions on Power Delivery*, Vol. 4, No. 1, 1989, pp. 141-56.
11. D. F. Crouse, P. Willett and Y. Bar-Shalom, "A low-complexity sliding-window Kalman FIR smoother for discrete-time models," *IEEE Signal Processing Letters*, Vol. 17, No. 2, 2009, pp. 177-80.
12. J. Sarmavuori and S. Sarkka, "Fourier-hermite kalman filter," *IEEE Transactions on Automatic Control*, Vol. 57, No. 6, 2011, pp. 1511-5.
13. L. Hong, G. Cheng and C. K. Chui, "A filter-bank-based Kalman filtering technique for wavelet estimation and decomposition of random signals," *IEEE Transactions on Circuits and Systems II: Analog and Digital Signal Processing*, Vol. 45, No. 2, 1998, pp. 237-41.
14. J. R. Macias and A. G. Exposito, "Self-tuning of Kalman filters for harmonic computation," *IEEE transactions on power delivery*, Vol. 21, No. 1, 2005, pp. 501-503.
15. L. Reggiani, L. Dossi, L. Barletta and A. Spalvieri, "Extended Kalman Filter for MIMO Phase Noise Channels With Independent Oscillators," *IEEE Communications Letters*, Vol. 22, No. 6, 2018, pp. 1200-1203.
16. K. Reif and R. Unbehauen, "The extended Kalman filter as an exponential observer for nonlinear systems," *IEEE Transactions on Signal processing*, Vol. 47, No. 8, 1999, pp. 2324-2328.
17. C. Pantaleón and A. Souto, "Comments on An aperiodic phenomenon of the extended Kalman filter in filtering noisy chaotic signals," *IEEE transactions on signal processing*, Vol. 53,No. 1, 2004, pp. 383-384.
18. Y. S. Shmaliy, "Suboptimal FIR filtering of nonlinear models in additive white Gaussian noise," *IEEE Transactions on Signal Processing*, Vol. 60, No. 10, 2012, pp. 5519-5527.
19. J. Zhao, M. Netto and L. Mili, "A robust iterated extended Kalman filter for power system dynamic state estimation," *IEEE Transactions on Power Systems*, Vol. 32, No. 4, 2016, pp. 3205-3216.
20. J. Havlík and O. Straka, "Performance evaluation of iterated extended Kalman filter with variable step-length," *In Journal of Physics: IOP Publishing Conference Series 2015*, 659 Doi:10.1088/1742-6596/659/1/012022.
21. J. Fang, X. Gong, Predictive iterated Kalman filter for INS/GPS integration and its application to SAR motion compensation, IEEE transactions on instrumentation and measurement. 59(4)(2009) 909-915.
22. A. Shademan and F. Janabi-Sharifi, "Sensitivity analysis of EKF and iterated EKF pose estimation for position-based visual servoing," *In Proceedings of 2005 IEEE Conference on Control Applications*, 2005, pp. 755-760.
23. A. H. Jazwinski, "Stochastic processes and filtering theory," *Courier Corporation*, 2007.
24. P. Stano, Z. Lendek, J. Braaksma, R. Babuska, C. de Keizer and J.Arnold, "Parametric Bayesian filters for nonlinear stochastic dynamical systems: A survey," *IEEE transactions on cybernetics*, Vol. 43, No. 6, 2013, pp. 1607-1624.
25. A. Bernardini, K. J. Werner, A. Sarti and J. O. Smith III, "Modeling nonlinear wave digital elements using the Lambert function," *IEEE Transactions on Circuits and Systems I: Regular Papers*, Vol. 63, No. 8, 2016, pp. 1231-1242.

AUTHORS PROFILE

Amit Kumar Gautam was born in Uttar Pradesh, India in the year of 1987. He got B.Tech. degree in Electronics and Communication Engineering from M.I.T. Moradabad (India) and M.Tech. degree in Signal Processing and Digital Design from Delhi technological University, New Delhi, India. He worked as senior research scholar (SRF) in Delhi technological University. His research interests is signal processing and circuit estimation.

Sudipta Majumdar received B.Tech. and M.Tech. degree from University of Allahabad. She received Ph.D. degree from Delhi University. She is working as Assistant Professor in Delhi Technological University from 2010. Her research interests include nonlinear analysis, signal processing and image processing.